



Qualification of gamma spectrometry measurement for the radiological characterization of mixed VLLW cables in particle accelerators

Maeva Rimlinger, Thomas Frosio^{*}, Nabil Mena, Matteo Magistris, Chris Theis

Radiation Protection Group, European Organization for Nuclear Research, 1211 Geneva 23, Switzerland

ARTICLE INFO

Keywords:

Gamma spectrometry qualification
Particle accelerators
Very-low-level radioactive waste
Mixed material characterization
Measurement uncertainty quantification

ABSTRACT

In the framework of maintenance activities in particle accelerators, such as upgrades and dismantling, a large number of activated equipment are removed from the accelerator complex and require characterization in view of their disposal as radioactive waste. In particular, cables can be of different types. This feature induces variations of the efficiency calibration curves due to the variation of the material composition, source distribution and density. Hence, quantifying the activities of the gamma-emitting radionuclides can be quite challenging for mixed cables. In this article, we propose a new qualification methodology, based on gamma spectrometry, in order to assess the activity results uncertainties of gamma-emitting radionuclides. This new methodology is developed to define the envelop efficiency calibration curves and allows for the establishment of more accurate activity values with their corresponding uncertainties.

1. Introduction and context

The purpose of the project “ELICA” (ELImination of very low-level waste (VLLW) Cables) is to establish the elimination pathway of VLLW cables towards the French repository. In the past, the elimination process targeted containers filled with cables that were sorted depending on the type of wire (aluminium or copper), and mass fractions of wire and insulation. The operations aimed at sorting require identification, handling and additional storage of cables which can be time and space consuming. In order to reduce the complexity of the process, the cable sorting operation has been eliminated allowing mixing the various cable types. A new characterization methodology was implemented in 2019, which allowed for the generation of waste packages with a mixture of aluminium and copper cables. Typical radionuclides encountered in the waste analysis are Co-60, Na-22, Ti-44 for instance.

The aim of the present document is to update and qualify new gamma spectrometry efficiency calibration curves for packages filled with mixed cables. It details the influence of the geometry parameters (such as the material composition, density and hotspots) on the values of the efficiency calibration uncertainties related to the ELICA project. This methodology is also applicable to other waste elimination campaigns projects. Therefore, it contributes to define the foundations of gamma spectrometry efficiency calibrations in a more rigorous and technically sound uncertainty analysis. The main component of the efficiency

calibration uncertainties originates from the parameter uncertainties of the geometry model. They have to be considered for gamma spectrometry measurements in order to accurately estimate the activity values. Any deviations between the “as calibrated” geometry and the “as measured” geometry contribute to the total uncertainty.

In section 2 of this document we provide the waste typology and characteristics. In section 3 we describe the measurement setup and the software tools used to estimate the efficiency calibration uncertainties. In section 4, we describe the qualification process we used in order to estimate efficiency calibration uncertainties. We then perform the uncertainty quantification in section 5. Finally, in section 6, we recommend a set of uncertainties to associate to each gamma spectrometry activity result.

2. Radioactive waste description

Within the frame of the ELICA elimination process there are five families of cables, each with different mass fractions of copper, aluminium and insulation (i.e., Polyvinyl chloride) (Fig. 1). These five families are now mixed within the same waste package.

On the one hand, we can estimate the relative amount of each family based on the feedback of previous cable eliminations (760 m³ of cables eliminated by doing single-family packages). On the other hand, we measured the mass fractions of copper, aluminium and insulation in

^{*} Corresponding author.

E-mail addresses: maeva.rimlinger@cern.ch (M. Rimlinger), thomas.frosio@gmail.com (T. Frosio).



Fig. 1. Samples of the five families of ELICA cables.

cables originating from the five families. From these two sets of data, we can build the typical ELICA typology of waste. The final result is summarized in Table 1, which presents the expected mass fractions for the three materials found in the five cable families and the associated uncertainties given at 1σ. The correlations between mass fractions are all negative (from -0.8 to -0.2). Hence, we decided in the next to neglect it in order to reduce uncertainty propagation framework. As correlations are negative, our proposed method remains conservative. Fig. 2 illustrates the final “products” of 1) the sorting process in the pilot project and 2) the current process that allows mixing cable families in the waste package.

In order to perform the uncertainty calculations, one needs to describe the geometry parameters that generate the efficiency calibration curves. In particular, the critical parameters in terms of uncertainties are:

- The material composition: Since the ELICA campaign currently allows for mixing cables, one needs to assess the impact of the variation of material composition (as described in Table 1) on the activity results.
- The material density: The efficiency calibration uncertainties need to take into account the mass variation ranges of the ELICA waste packages. Since the waste packages are now mixed with materials having different densities, from insulation to copper, their masses could vary considerably. The feedback from the pilot project shows that the net weight of the cable waste packages ranges from 600 kg to 2500 kg. The mass variation impacts the variation of apparent density, which in turn affects the gamma attenuation within the matrix.
- Hotspots or heterogeneous source distribution: Each waste package is likely to have one or several hotspots with different sizes and source concentrations. This is a parameter which cannot be operationally controlled and identified. Therefore, it is required to be taken into account in the uncertainty analysis.

3. Gamma spectrometry setup

3.1. ISOCS & LabSOCS

ISOCS (In Situ Counting Object System) and LabSOCS (Laboratory Sourceless Calibration Software) from Mirion technologies (Canberra) are used for creating efficiency calibrations (Venkataraman et al., 2003) (Menaet. al., 2011). In the software, the user selects the characterized detector from a list of available detectors, and indicates the sample geometry (i.e. the location and physical properties of the item being measured and the location and distribution of the source). The software does not require any additional information relating to the detector itself, this information is automatically extracted from a detector characterization file that is generated through the manufacturer’s characterization process. An example of the ISOCS model is shown in Fig. 3. The detectors at CERN undergo a commissioning phase following

Table 1
Expected mass fractions of sampling a cable from the packages for each material and corresponding standard deviation.

Material	Expected mass fractions (%)
Copper	44.0 ± 5.3
Aluminium	4.5 ± 1.4
Insulation	51.5 ± 8.6



Fig. 2. Picture of a waste package from the pilot process (cables sorted by family, left) and from the current process (mixed cables, right).

the standard (Standard Test Proced, 1109).

3.2. ISOCS Uncertainty Estimator - IUE

To create an ISOCS calibration file, one needs to know the physical parameters of the object, such as dimensions and composition of the waste package and sample. Some of those parameters are well known and do not vary appreciably; e.g., the container is always known to be type 304 stainless steel. Other parameters are not-well-known, e.g., the hotspots or the material composition of the content. As the geometry parameters are not well-known, strong assumptions are needed to be taken regarding their variation ranges using the best knowledge. Moreover, we have observed, from previous studies, that these parameters contribute to the efficiency uncertainty budget (Frosio et al., 2020a).

A tool named ISOCS Uncertainty Estimator (IUE) (Bosko et al., 2011) (Spillane et al., 2010)(Bronson, 1997) has been developed by Mirion Technologies (Canberra) to improve the quality and traceability of the gamma spectrometry uncertainty estimation by generating perturbed model efficiencies. IUE samples the geometry parameters within the input ranges to generate an efficiency calibration starting from the reference set of parameters. In a sense, it perturbs the reference model by varying the parameters around the reference values. It is worth noting that the interval can be continuous for continuous parameters (such density, filling height, ...) or discrete (such as material type).

The user first runs the ISOCS software in the usual manner to compute the reference efficiency for the sample being measured. For each not-well-known parameter, the user is required to provide an estimate of the parameters’ variation intervals; e.g., by measuring a group of containers or consulting the manufacturing specifications for the containers or just by making educated guesses (also called expert elicitation). The parameters that can be varied include dimensional parameters (diameter, distance, thickness, density, etc.), as well as material composition of each item of the model. For each not-well-known parameter the user provides upper and lower limits (e.g., maximum and minimum density) and a distribution form that the parameters are assumed to follow within those limits. An example of IUE interface is

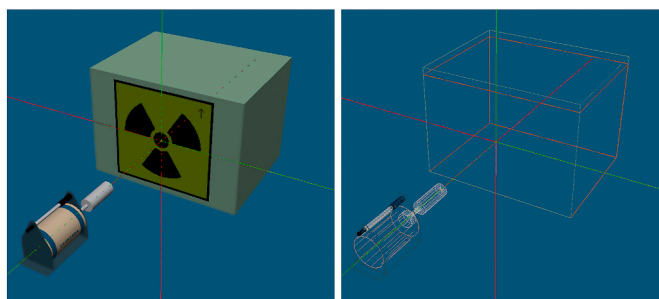


Fig. 3. ISOCS 3D model of the reference geometry.

provided in Fig. 4.

3.3. Geometry uncertainty reduction utility - GURU

The output of IUE is a collection of models efficiencies and parameters in four separate files: “.GIS,.ECC,.UGS, and .UEC”. We developed a Data Analyzer framework named “GURU” (Frosio et al., n.d.), which compares the output of IUE for a set of gamma spectrometry measurements performed in different positions on the same object. GURU has two modules. One module, named spectroMatcher, that allows finding a “best geometry model” based on multi-count and multi-line consistency techniques. This module is not used in the present paper. The second module, named DataAnalyzer allows correlating the geometry model parameters to the efficiency calibration curves. The previously mentioned group of models are combined within the GURU framework. Then, it computes the absolute and relative sensitivities of efficiency calibration curves compared to the reference geometry model.

3.4. Detectors characteristics

The gamma spectrometry measurements are performed in a dedicated laboratory. It is equipped with two High Purity Germanium detectors (Falcon 5000 HPGe)¹ on each side of the room as shown in Fig. 5. Each detector undergoes an on-site commissioning and a quality assurance program to verify continuous quality and reliability during the detector’s use and operation. Our Quality-Assurance program is inspired from the ISO/IEC 17025². A system background subtraction of each gamma spectroscopy analysis is performed via GENIE 2000 software. The distance between package and detector is measured by a BISCH laser range finder³ with an uncertainty of ± 2 mm.

3.5. Reference efficiency calibration geometry

The present study focuses on waste packages filled with radioactive waste consisting of cables. The physical and chemical characteristics for this reference waste package are shown in Table 2 and the corresponding ISOCS/LabSOCS geometry model is shown in Fig. 3.

To create the reference ISOCS calibration curve, one needs to know the physical parameters, such as the dimensions of the waste package, the radioactive waste and the composition. The model based on these reference parameters will be denoted as reference model in the rest of this document. The waste package shown in Fig. 2 is simulated using the ISOCS/LabSOCS 3D geometry composer with the “Complex Box” template, of which the parameters are described in Fig. 6.

The detector-to-waste package distance is set to 750 mm. The material density is derived from the waste package net weight after subtracting the empty waste package weight. In the reference model, the density is set to 0.683 g/cm³. The density of 0.683 g/cm³ could appear low for copper cables. It has to be understood by the reader that it is an apparent density that takes into account the presence of air and material with less density than copper.

4. Qualification process

Qualification is a process used to evaluate the capacity of a model to predict physical quantities (in our case, the efficiency of the gamma spectrometry measurement) within a set of assumptions. The aim is to quantify random errors and biases of a simplified, reference model. It is generally achieved by comparing this simplified reference model with

an optimized experimental model considered as the “best model”, which represents the best knowledge we can have regarding a system.

In this study we do not have one single “best model”, because the apparent density of waste packages varies depending on the exact mixture of cables, which leads to a variety of possible geometry models. We therefore decided to investigate the efficiency values variation of the various geometry models. The various geometry models are constructed in order to estimate the efficiency uncertainties. The input parameters are perturbed considering the assumed geometry parameters uncertainties. The efficiency calibration curves of these perturbed models are collected and their variations are analyzed. Finally, we consider as the best model the “envelop model”, i.e. the geometry model that provides lower limits for efficiency at a confidence level of 95%. It should be noted that a lower value of efficiency leads to a higher predicted value of activity.

Hereafter a description of the semantics used within the document and corresponding mathematical equations (Fig. 7) will be shown.

In the rest of this document, the bias (M 1995 and Evaluation of m, 2008) B of a reference model corresponds to the difference between the expected value of the reference model and the mean value of the various geometry models. The standard deviation (σ) quantifies the random error around the mean value of the various geometry models (ratio with the reference model). Both, bias and standard deviation, are expressed in relative terms throughout the following discussion.

The relation between the value of the envelop model $\varepsilon_p(E)$ and the value of the reference model $\varepsilon_0(E)$ is described in Equation (1) by means of a correction factor CF , where $CF = B + k\sigma$.

We here define the envelop value $\varepsilon_{Env}(E)$ as the lower value comparing the value of the envelop model $\varepsilon_p(E)$ and the value of the reference model $\varepsilon_0(E)$. Indeed, if the mean value of the various geometry models is higher than the expected value of the reference model, then the correction factor CF can be positive. In this case, the envelop value $\varepsilon_{Env}(E)$ is set to be equal to the value of the reference model $\varepsilon_0(E)$.

$$\varepsilon_{Env}(E) = \varepsilon_p(E) = \varepsilon_0(E) (1 + CF) \quad \text{if } CF < 0$$

$$\varepsilon_{Env}(E) = \varepsilon_0(E) \quad \text{if } CF > 0 \quad (1)$$

Equation (1): Relation between the envelop value, the expected value of the envelop model and the expected value of the reference model.

In the rest of this document, we aim at identifying the systematic and random errors in order to take them into account during routine gamma spectrometry analyses of ELICA waste. Based on the waste typology (measurements in waste package, masses range, activity heterogeneity, material), it is possible to group the sets of waste in order to associate a reasonably small uncertainty with the activity results. This uncertainty will have to be considered and applied to the activity results when using the reference model.

Once the uncertainties on the efficiency calibration curve are defined, one needs to include them in the uncertainties of the activity results. One method consists of updating the uncertainties directly into ISOCS/LabSOCS software before calculating the efficiency curves. This is the process we consider in this document. Alternatively, one could also include those uncertainties directly in the final activity results.

5. Efficiency calibration variation

This section aims at estimating the calibration efficiency uncertainties (Frosio et al., 2020a) that are due to the following geometry variation parameters:

- Material composition
- Waste density,
- Activity heterogeneity (or activity distribution within the waste package).

¹ http://www.canberra.com/fr/produits/hp_radioprotection/falcon-5000.asp.

² ISO/IEC 17025 General requirements for the competence of testing and calibration laboratories.

³ <https://www.bosch-professional.com/ch/fr/products/glm-30-0601072502>.

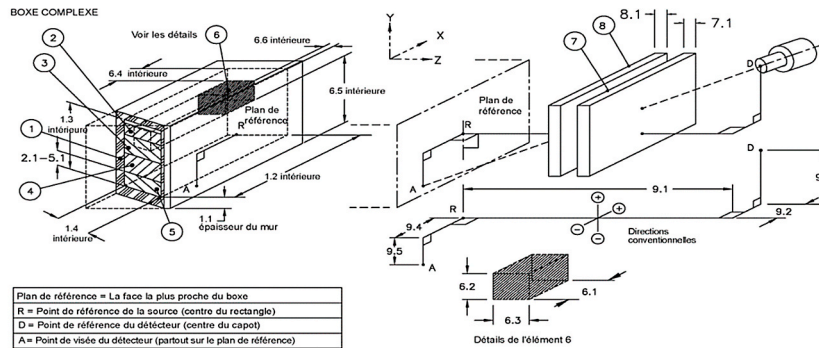
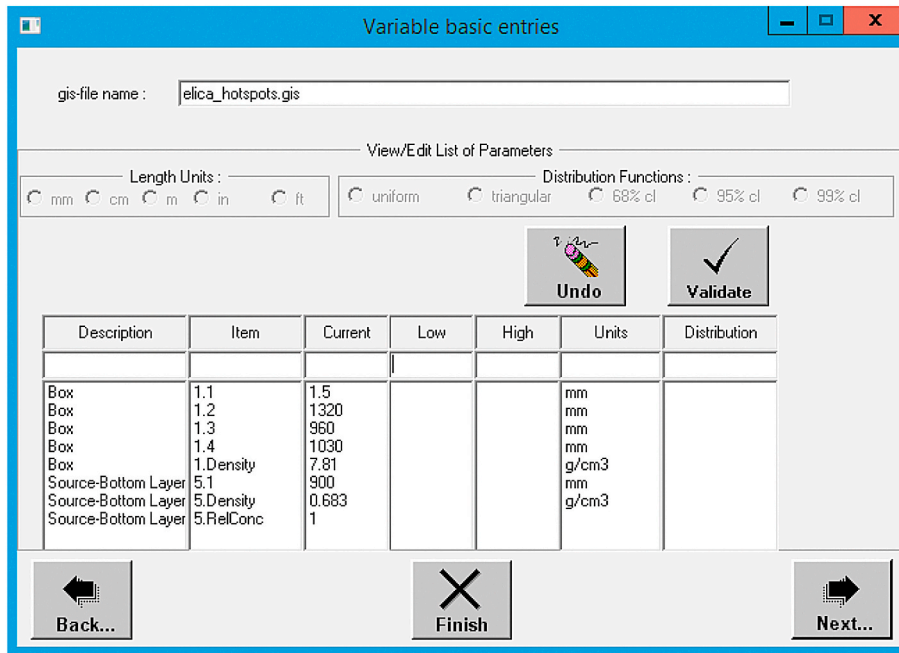


Fig. 4. Typical IUE data input screen. Parameters are entered in the top window to describe the amount and type of variation for the model. The bottom window details the complex box template geometry parameters.



Fig. 5. Gamma spectrometry performed in a dedicated area. The white marks on the floor represent the location of the waste package.

In order to study the effect of the variation of the material composition, densities and possible matrix heterogeneities, IUE computations are performed. 1000 efficiency calibration curves are randomly generated, by separately perturbing density and heterogeneity parameters of

Table 2

Physical and chemical characteristics of the reference ISOCS model.

Container height, length, width (mm)	960 × 1320 x 1030
Container thickness (mm)	1.5
Radioactive waste dimensions (mm)	900 × 1320 x 1030
Empty container mass (kg)	190
Chemical composition of the waste package	304 Stainless steel: 100.00%
Chemical composition of the radioactive waste	Copper 44.00%, Aluminium 4.50%, PVC 51.50% (see Table 1)

the geometry model according to their estimated probability distribution. Regarding the material composition, 100 models are generated to simulate probable mixtures of cable families.

5.1. Influence of the material composition

5.1.1. Material sampling: compositional data fitting with a dirichlet distribution

Material composition is here considered as a set of statistical variables. In order to study the efficiency response variation, we perform a random sampling of 100 material compositions propagated into IUE. The material compositions of the waste packages present two

No.	Description	d.1	d.2	d.3	d.4	d.5	d.6	Material	Density	Rel. Conc.
1	Boite	1.5	1320	960	1030			304ss	7.81	
2	Source - Couche	0							0	0.00
3	Source - Couche 2	0							0	0.00
4	Source - Couche 3	0							0	0.00
5	Source - Couche	900						elica	0.683	1.00
6	Source - Source	330	225	257.5	495	337.5	386.25	elica	0.683	1.00
7	Absorber 1	0							0	
8	Absorber 2	0							0	
9	Source-Detector	750	0	0	0	0				

Fig. 6. Efficiency calibration geometry parameters for the reference model using the Complex Box template.

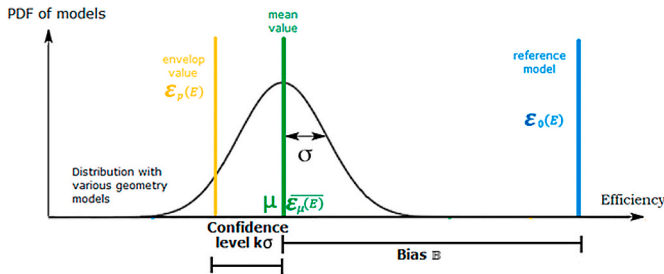


Fig. 7. Schematic representation of the parameters involved in the qualification process.

constraints:

- They are continuous, positive, and multivariate data,
- Their sum must be equal to 1.0.

A mathematical framework exists in the literature to represent such kind of data. It is named ‘‘Compositional data’’ (Rodrigues et al. et al., 2011) and is usually described via the Dirichlet distribution (Hijazi and Jernigan, 2009)(Aitchison, 2003).

Our strategy is to model the generic ELICA material composition (cf section 2) based on the Dirichlet distribution. Due to the constraint on the variable (mass fractions of the material compositions) sum to be equal to 1, it is convenient to define these variables on the standard simplex. The n-simplex is a Euclidian space of n+1 linearly independent points. Geometrically, it is the generalization of the triangle to n dimensions. The standard simplex ζ is formed of the n+1 standard unit vectors and is defined in Equation (2).

$$\zeta = \left\{ x \in \mathbb{R}_+^{n+1}, \sum_i x_i = 1, x_i \geq 0, i = 1..n + 1 \right\} \quad (2)$$

Equation (2): Definition of the standard simplex.

In this study, we consider the Dirichlet distribution of order 3, denoted $Dir(\bar{\alpha})$. The distribution is parameterized by the vector of positive real numbers $\bar{\alpha} = (\alpha_1, \alpha_2, \alpha_3)$. The Dirichlet distribution is the multivariate version of the beta distribution, in the same way that the multinomial distribution (its conjugate prior) is the multivariate version of the binomial distribution. For this reason, when the order of the Dirichlet distribution is 2, it becomes a beta distribution.

The moments of first and second orders for a Dirichlet variable $X = (X_1, X_2, X_3)$ are expressed in Equation (3), where $\alpha_0 = \sum_{k=1}^3 \alpha_k$.

$$\begin{cases} E[X_i] &= \frac{\alpha_i}{\alpha_0} \\ Var[X_i] &= \frac{\alpha_i(\alpha_0 - \alpha_i)}{\alpha_0^2(\alpha_0 + 1)} \\ Cov[X_i, X_j] &= \frac{-\alpha_i\alpha_j}{\alpha_0^2(\alpha_0 + 1)} \end{cases} \quad (3)$$

Equation (3): Expression of the mean, variance and covariance, for a Dirichlet distribution.

In particular, Equation (3) shows that the expectation of the marginal (beta distributions) is the fraction of its parameter with respect to the total sum of the marginal parameters.

The α_i values affect the shape of the Dirichlet distribution over the following:

- The higher value of α_i , the more dense is the distribution. Hence, a greater amount of the total mass is assigned to its marginal. On the opposite, when $\alpha_i < 1$, the distribution is more sparse and the corresponding x_i values are pushed to the extremities of the graph.
- If all α_i are equal, the distribution is symmetric, in the meaning it is evenly distributed.
- If $\alpha_1 = \alpha_2 = \alpha_3 = 1$, then the x_i values are uniformly distributed.

Due to the high variation of shapes of the distribution, with $\bar{\alpha}$ values variations, the Dirichlet distribution is often used for Bayesian inference, as conjugate prior.

The estimation of the $\bar{\alpha}$ parameter of the Dirichlet distribution is here performed by the Method of Moments (MM) which is reasonably simple while yielding consistent estimators. We consider k moments of first order and k moments of second order. As we need to solve the equation system for k unknowns, we construct an equation system containing:

- k-1 equations from the first order moments,
- One equation from the second order moments.

We then derive the associated system of equations (Equation (4)) and its solution (Narayanan, 1992) (Equation (5)). This method identifies the parameter which best fits the set of observed data (summarized in Table 1). As a result, in the rest of this document, the considered $\bar{\alpha}$ parameter is given in Equation (6).

$$\begin{cases} \forall i = 1..k - 1, E[X_i] = \frac{\alpha_i}{\alpha_0} \\ E[X_k^2] = Var[X_k] = \frac{\alpha_k(\alpha_k + 1)}{\alpha_0(\alpha_0 + 1)} \end{cases} \quad (4)$$

Equation (4): Equation system to express the $\bar{\alpha}$ parameter of the Dirichlet distribution

$$\begin{cases} \forall i = 1..k - 1, \alpha_i = \frac{[E[X_1] - (Var[X_1] + E^2[X_1])]E[X_i]}{Var[X_1]} \\ \alpha_k = \frac{[E[X_1] - (Var[X_1] + E^2[X_1])] \left(1 - \sum_{i=1}^{k-1} E[X_i]\right)}{Var[X_1]} \end{cases} \quad (5)$$

Equation (5): Solution of the equation system (method of moments).

$$\bar{\alpha} = \left(\underbrace{17.36}_{\text{Insulation}}, \underbrace{14.80}_{\text{Copper}}, \underbrace{1.52}_{\text{Aluminum}} \right) \quad (6)$$

Equation (6). The parameter $\bar{\alpha}$ of the Dirichlet distribution.

An illustration is available in Fig. 8. The left figure represents a random process for 20 000 mass fractions sampled in the $Dir(17.36, 14.80, 1.52)$. We produce a set of 100 compositions in this distribution (right part of Fig. 8). These mass fractions are used in the next section 5.1.2 in order to assess efficiency calibration uncertainties due to the material variation. We can see in Fig. 8 that the variation domain of the composition is limited to the right part of the ternary diagram, due to the low quantities of aluminium encountered in the cable families.

Considering the 100 compositions, the copper, aluminium, and insulation mass fraction histograms are plotted in Fig. 9. One can see that the corresponding means are consistent with the experimental

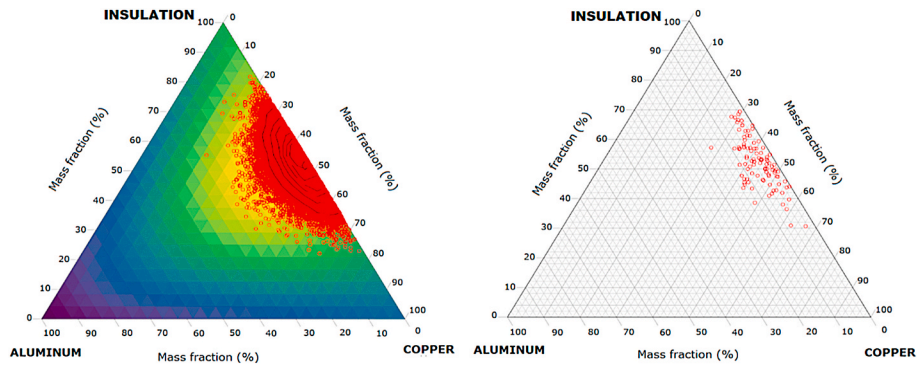


Fig. 8. Ternary diagrams of mass fractions (copper, insulation, aluminium) in the ELICA waste composition. Left figure is an illustration of the domain area of the Dirichlet distribution. Right figure presents the 100 compositions considered in this document for assessing efficiency calibration uncertainties originating from material composition.

values shown in Table 1. Regarding the standard deviation, some slight differences can be noticed. A minor overestimation of the standard deviation is observed, due to the Dirichlet fitting process (e.g. 7.9% for copper instead of the measured 5.3%). Hence, the efficiency calibration uncertainties originating from material composition will be slightly overestimated. The main message is that the 100 random samples are representative of the measured values, when modelled by the $Dir(17.36, 14.80, 1.52)$ distribution.

5.1.2. Efficiency uncertainty results

The reference model is based on the average composition detailed in Table 1. In order to assess the efficiency calibration variations for mixed cables, 100 models are generated (Fig. 8) and simulated with ISOCS. In these models, only the material composition is varied.

Fig. 10 shows the relative difference of the efficiency curves of the perturbed models compared to the reference model, described in Equation (7), where $\epsilon_i(E)$ is the full peak efficiency value at energy E for the model i, and $\epsilon_0(E)$ is the reference full peak efficiency value at energy E in the model i.

$$R(E, \%) = \frac{\epsilon_i(E)}{\epsilon_0(E)} - 1 \tag{7}$$

Equation (7): Relative difference of the efficiency values of the perturbed models compared to the reference model.

At 45 keV, the influence of the material composition is the highest. In other words, overestimating the copper content causes the overestimation of the efficiency values using the uniform model by a maximum of 32.44% (hence, underestimate the activity values). On the opposite, increasing the aluminium content in the waste package (or minimizing the copper fraction), causes the underestimation of the efficiency using the uniform model by a maximum of 41.37% (which leads to higher activity values).

These results are interesting to consider for low gamma emitter such as the actinide radionuclides or for measuring background with Th-232.

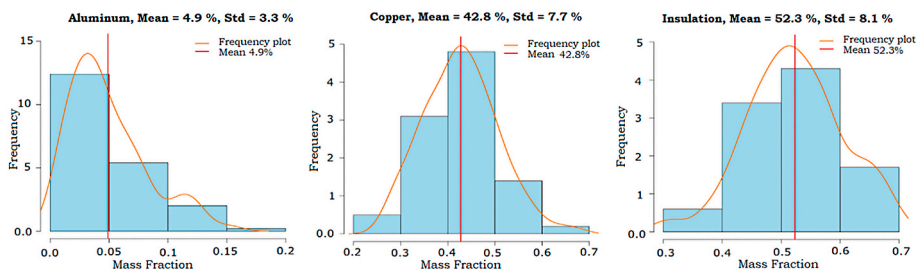


Fig. 9. Distributions of the copper, aluminium, and insulation mass fractions in the 100 material compositions sampled in the Dirichlet distribution. From left to right: aluminium, copper and insulation.

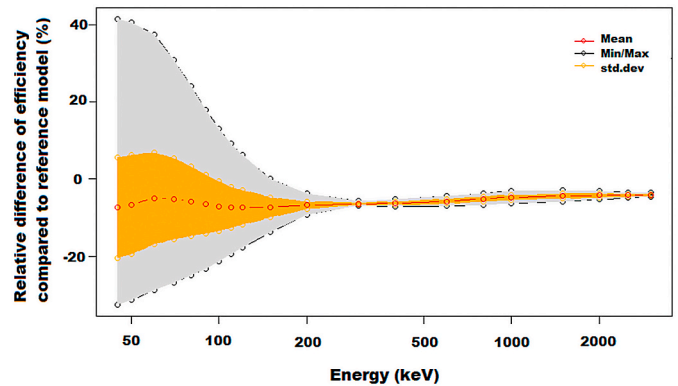


Fig. 10. The relative efficiency difference compared to the reference model from 45 keV to 3000 keV.

For the purpose of the ELICA study, the radionuclides of interest have gamma rays with energies above 120 keV (Co-57 ray at 122 keV) or above 1 MeV for the key radionuclides such as Co-60 and Sc-44. Hence, the variation of the elemental composition does not present an important contribution to the total uncertainty budget. On the other side, this study shows that the uncertainties that are due to the elemental composition could be important for waste characterizations that contain actinides and transuranic nuclides with gamma ray energies below 120 keV.

The activity uncertainty value that is due to the material composition includes two components:

- 1) The bias between reference and the perturbed model for the systematic terms,
- 2) The random uncertainties considered at 1σ . The uncertainty values are summarized in Table 3.

In Table 3, we also compare the materials used during the pilot project of ELICA (50% copper with 50% insulation and 50% aluminium with 50% insulation) to the current reference model.

5.2. Impact of the density variations

The density and the mass of the waste packages are correlated by the waste package’s volume which is fixed during the whole analysis. Therefore, for operational reasons (mass measurement is more practical than density) we consider in this section the impact of the mass variations of the waste package on the efficiency calibration values. In order to assess this impact, we perform a sensitivity study. Furthermore, in order to improve the uncertainty estimation, the sensitivity analysis is done for 20 different material compositions.

An illustration of the efficiency variation as a function of the mass is available in Fig. 11.

The sensitivity coefficients $S(E, \%)$ are expressed as the relative efficiency calibration difference at a specific energy E per relative mass difference (Equation (8)), where X represents the average over the i perturbed models, $\varepsilon_i(E)$ is the efficiency calibration at energy E for model i and m_i is the corresponding waste mass in model i .

$$S(E, \%) = \left(\frac{\varepsilon_{i+1}(E)}{\varepsilon_i(E)} - 1 \right) / \left(\frac{m_{i+1}}{m_i} - 1 \right) \quad (8)$$

Equation (8): Sensitivity coefficient of the efficiency calibration to the mass.

The average and standard deviation values for the sensitivity coefficient at energies ranging from 45 keV to 3 MeV are shown in Table 4.

The average relative sensitivity is stable as a function of energy. Its value ranges from -0.9% at 45 keV to -0.7% at 3 MeV (per unit percent variation of the mass). The corresponding standard deviation, however increases from 0.06% at 45 keV to 0.15% at 3 MeV. As the sensitivity coefficient is negative, a positive variation of mass induces a negative variation of the efficiency. Consequently, a positive variation of mass induces a positive variation of activity result. Hence, this has to be considered in order to avoid underestimation of the activity values. In the next, for simplification of the results, we consider a sensitivity coefficient value of $-1\%/%$ (or -1% variation in efficiency for each $+1\%$ variation of density) in order to remove the energy dependence.

The objective is to construct efficiency calibrations for different mass ranges that will be operationally used according to the measured mass of

Table 3

Efficiency uncertainties due to the material composition variation. Values in percentage (CF coefficient) at 1σ .

Energy (keV)	Bias (%)	Standard deviation (%)	Relative difference R(50% Cu 50% PVC)	Relative difference R(50%Al 50% PVC)
45	-7.39	13.09	-14.79	259.52
50	-6.58	12.79	-13.02	237.35
60	-4.94	11.90	-10.01	189.55
70	-5.14	10.48	-7.70	146.13
80	-5.77	8.99	-5.61	112.27
90	-6.53	7.59	-3.86	86.99
100	-7.00	6.38	-2.33	68.42
110	-7.27	5.34	-3.52	48.55
120	-7.32	4.48	-2.67	38.63
150	-7.33	2.59	-1.45	20.39
200	-6.72	0.96	-0.60	8.15
300	-6.38	0.23	-0.48	0.98
400	-6.28	0.43	-0.56	-0.97
600	-5.74	0.55	-0.78	-2.17
800	-5.15	0.61	-0.96	-2.60
1000	-4.72	0.64	-1.11	-2.79
1500	-4.37	0.58	-1.28	-2.79
2000	-4.23	0.45	-1.50	-2.47
2500	-4.16	0.31	-1.78	-2.06
3000	-4.09	0.19	-2.03	-1.60

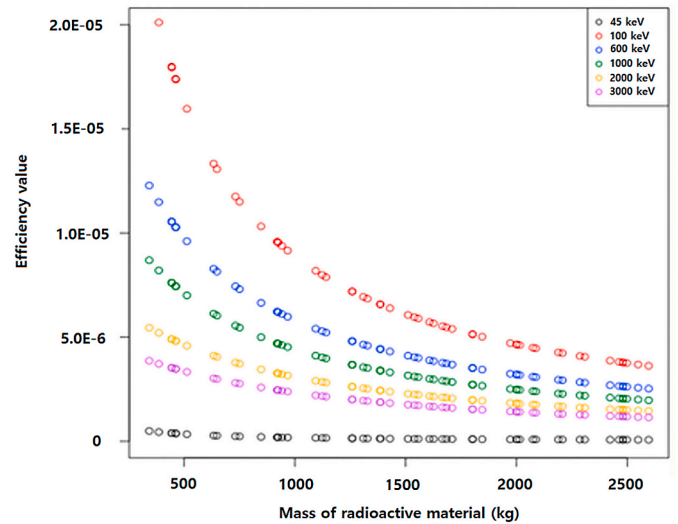


Fig. 11. Efficiency calibration at different energies as a function of the waste mass.

Table 4

Average and standard deviation values of the sensitivities (defined in Equation (8)) for different energy ranges up to 3 MeV.

Energy range	45 keV–70 keV	80 keV–120 keV	150 keV–200 keV	3 MeV
Average	-0.9	-0.9	-0.9	-0.7
Standard deviation	0.06	0.07	0.08	0.15

the package. This set of curves will be considered in the measurement process. The package will be weighted and the curve corresponding to the package mass will be used (see section 6). We target a maximum uncertainty of 10% on the efficiency value, from the mass variation. The feedback from ELICA pilot project set a minimum filled waste package mass at 600 kg. Thus, the total number of curves between 600 kg and 5000 kg (maximum) is set at 15. Table 5 shows the list for each range of mass and their total relative sensitivity.

5.3. The hotspot uncertainty or the activity heterogeneity impact

Activation mechanisms highly depend on the location in the accelerators. As we are mixing different cables, they can have different activation profiles. Hence, the waste package can present activity distribution heterogeneities as seen for VLLW magnets in (Frosio et al., 2020b). The following section focuses on the impact of such heterogeneities in the spatial distribution of radionuclides within the waste package.

5.3.1. Model description and characteristics for the hotspot variations

In what follows, we vary the activity distribution by varying the following hotspot parameters: dimensions, source relative concentration and locations within the waste package. The waste package size remains identical as listed in Table 2. The hotspot parameters are described in Table 6. The reference model consists of a centered hotspot with a relative concentration 1 compared to the rest of the waste matrix.

We constructed a set of 1000 perturbed geometry models by varying the dimensions, locations, relative concentrations and the number of the hotspots. The hotspots can be located in the whole waste package with physical dimensions varying from $33 \times 22.5 \times 27.75 \text{ cm}^3$ (25% of the maximum waste dimension) to $132 \times 90 \times 103 \text{ cm}^3$. The relative

Table 5

Efficiency calibration curves for different mass ranges and associated maximum error (considered as uncertainty at 2σ in the next of the document). Note the bias for the density variation is null since the reference model is centered for the various mass ranges.

Curve number	Reference mass (kg)	Range of mass (kg)	Maximum error on the efficiency (or uncertainty at 2 sigma) (%)
1	650	600–700	8.3%
2	750	700–800	7.1%
3	850	800–900	6.3%
4	950	900–1000	5.6%
5	1100	1000–1200	10.0%
6	1300	1200–1400	8.3%
7	1500	1400–1600	7.1%
8	1700	1600–1800	6.3%
9	1900	1800–2000	5.6%
10	2200	2000–2400	10.0%
11	2600	2400–2800	8.3%
12	3000	2800–3200	7.1%
13	3500	3200–3800	9.4%
14	4100	3800–4400	7.9%
15	4700	4400–5000	6.8%

concentration and the number of random hotspots can vary from 1 to 5 times compared to the rest of the waste package. The characteristics of the IUE settings are shown in Fig. 12.

5.3.2. Efficiency uncertainty results

The first 1000 IUE calculations are established using a mass of 1000 kg. Once the IUE calculations are performed, we use GURU (see section 3) to increase the initial 1000 models 8 times, by varying the hotspot relative concentrations. This step allows for overcoming the IUE limitation of varying this parameter.

The first results, in Fig. 13, show the relative efficiency with one germanium detector. As expected, the influence of the unknown activity distribution is non negligible. It represents a new challenge in defining a reasonable penalizing geometry.

These results show the uncertainty applied for one detector in the presence of hotspots within the waste package. However, operationally, each waste package is measured on each side as seen in section 3.

In order to assess the activity ratio of the two detectors, we consider our feedback using four ELICA waste packages that were already measured and analyzed using the gamma spectrometry technique. The waste packages with the highest masses are selected as they induce higher uncertainties on the activity values when perturbing the hotspots parameters (i.e. waste package masses around 2650 kg).

In case hotspots would be an important issue, performing a tomographic scan of the waste to solve the inverse problem and then reconstruct the hotspots characteristics could be considered (Dumazert et al., 2020)(Carrelet et al., 2014).

Tables 7 and 8 give the activity ratio measured for each waste package. We see that the contrast between two opposite faces is always below 3, confirming the choice of the hotspots concentration variation interval from the rest of the waste matrix. Moreover, the identified radionuclides allow for covering the whole energy range of the efficiency calibration (from 122 keV to 1.7 MeV). The efficiency uncertainties are summarized in Table 9.

Table 6

Hotspot characteristics in the ISOCS “Complex box” template for the reference model.

Details on the hotspot in the reference model									
Parameter reference	6.1 ^a (mm)	6.2 (mm)	6.3 (mm)	6.4 (mm)	6.5 (mm)	6.6 (mm)	Material reference	Rel. Conc.	Number of hotspots
Value	330	225	257.5	495	337.5	386.3	reference	1.0	1

^a See Fig. 4 for correspondences between numbers and geometry parameter. For instance, 6.1, 6.2 and 6.3 refer to the hotspot dimensions while 6.4, 6.5 and 6.6 refer to the hotspot location.

6. Recommended Calibration efficiency curves using total uncertainty estimation

After studying each uncertainty source due to each parameter variation, we can now include a systematic error (bias) and a random uncertainty for each defined mass range described in Table 5. Table 10 and Table 11 summarize these results as a function of energy. The total bias represents the sum of the individual biases while the total uncertainty is evaluated by the quadratic sum of the individual uncertainties originating from sections 5.1, 5.2 and 5.3.

In order to take into account the uncertainties described in this document, a set of 15 efficiency calibration curves is generated, according to the 15 discretization of masses of the waste package (section 5.2). Each efficiency curve is modelled with ISOCS considering the reference model:

- Uniform source distribution within the waste package,
- Expected material composition (see Table 1),
- Reference mass (see Table 5).

From each of the 15 efficiency calibration curve files generated, we modify the efficiency calibration and associated relative uncertainty at 1 sigma. The Bias is applied to the efficiency values $\epsilon_0(E)$ of the reference models (see Equation (9)). Then, the efficiency corrected from the bias is replaced (denoted here $\epsilon_\mu(E)$ as it represents the expectation model).

$$\epsilon_\mu(E) = \epsilon_0(E)(1 + B) \quad (9)$$

Equation (9): Correction of efficiency in the efficiency calibration curve file to take into account the bias.

In Equation (1), we establish the uncertainty (denoted $k\sigma$) as normalized by the reference model. Then, we express this uncertainty normalized to the expectation model (denoted μ in Fig. 7). This requirement comes from the efficiency calibration curve file. The efficiency uncertainty has to be linked to the efficiency value in this file. As we correct it from the bias and express the expected efficiency, we need to express the corrected uncertainty (denoted σ_μ) as a percentage of the bias-corrected, expected efficiency. We then derive Equation (10).

$$k\sigma_\mu = k \frac{\epsilon_0(E)}{\epsilon_\mu(E)} \sigma = k \frac{\sigma}{(1 + B)}, k = 1 \quad (10)$$

Equation (10): Correction of efficiency in the efficiency calibration curve file to take into account the uncertainty (expressed at 1 sigma).

We sum this uncertainty $k\sigma_\mu$ quadratically with the intrinsic efficiency uncertainty described to replace the one of the efficiency calibration curve file.

7. Conclusion

This study demonstrates a novel qualification methodology to estimate the gamma activity results of the ELICA waste packages based on the gamma spectrometry technique. The ELICA waste package is characterized by the variability of the material density, material composition, and activity heterogeneity.

For the material composition, the relative efficiency uncertainty varies from 4.5% at 120 keV to 0.6% at 1 MeV. In addition, the bias is also relatively small, decreasing from -7.3% at 120 keV to less than -5.0% at 1 MeV because the perturbed models vary around the centered

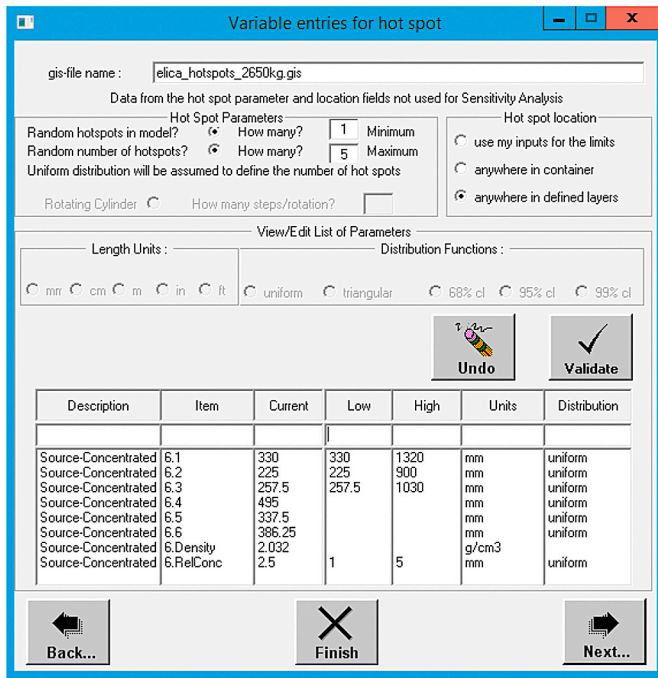


Fig. 12. IUE settings for the hotspot calculation for the 1000 kg configuration.

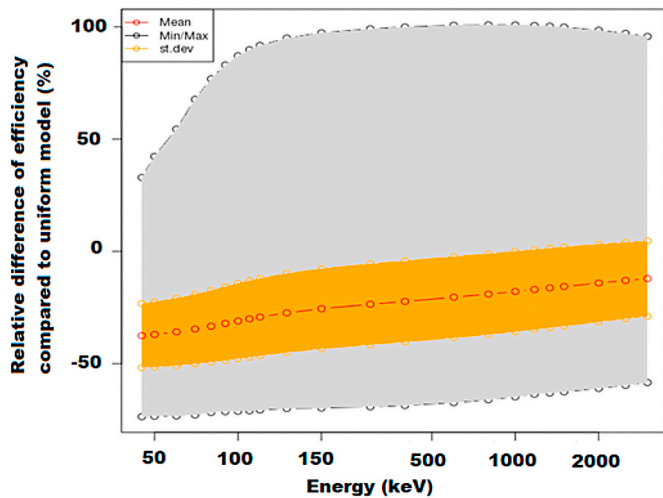


Fig. 13. Relative efficiency value compared to the reference model for one detector measurement.

reference model. For the purpose of the ELICA study, the radionuclides of interest have gamma rays with energies above 120 keV (Co-57 ray at 122 keV) or above 1 MeV for the key radionuclides such as Co-60 and Sc-44. Hence, the variation of the elemental composition does not present an important contribution to the total uncertainty budget. On the other side, this study shows that the uncertainties that are due to the elemental composition could be important for waste characterizations that include actinides and transuranic nuclides with gamma ray energies below 120 keV.

The results show also that the activity heterogeneity has a more significant impact on the correction factors. The efficiency standard deviation ranges from 21% at 45 keV to 18% at 1 MeV. Moreover, the corresponding bias is also higher with values going respectively from -39% to -20% at 1 MeV. The higher bias originates from the addition of hotspots which are not present in the reference model.

The final contributor to the correction factor is the density variation.

Table 7

Activity ratios of the two sides per gamma lines of each waste package for around 1000 kg waste packages.

Radionuclides	Energy line (keV)	P8-422	P8-462	P8-469	P8-494
Na-22	1274	1.01		0.97	0.93
Mn-54	834	1.26			
Co-57	122	1.45			
Co-58	810	1.52			
Co-60	1173	1.13	1.08	1.28	1.02
	1332	1.18	1.00	1.13	0.66
Sb-124	602	2.81	0.45		
	1690	2.71			

Since the objective is to construct efficiency calibrations for different mass ranges that will be operationally used according to the measured mass of the waste packages, we target a maximum error of 10% on the efficiency value, due to the mass variation. For this purpose, 15 efficiency calibration curves are generated depending on the mass range of the package.

The impact of all the parameters, on the activity results, is studied and a set of systematic and random errors is produced for all waste packages for each corresponding masse range. A set of correction factors are also recommended to define an upper limit of the efficiency values at 95% confidence level (2σ).

The uncertainty analysis shows that using one detector for spectrometry measurements induces high efficiency uncertainties due to the activity heterogeneity of the waste package. For instance, the efficiencies of the perturbed models differ from the reference model by about 25% at 1 MeV.

Table 8

Activity ratios of the two sides per gamma lines of each waste package for the 2650 kg waste packages.

Radionuclides	Energy line (keV)	GK-949	GK-953
Na-22	1274	0.97	0.71
Mn-54	834	1.56	0.76
Co-57	122	1.37	0.80
Co-58	810	1.81	0.80
Co-60	1173	1.15	0.87
	1332	1.20	0.87
Zn-65	1115	1.23	0.85

Table 9

Efficiency uncertainties coming from heterogeneities within the waste package matrix (1σ).

Energy (keV)	Bias (%)	Standard deviation (%)
45	-38.93	13.91
50	-38.42	14.15
60	-37.28	14.67
70	-36.07	15.15
80	-34.83	15.60
90	-33.63	16.03
100	-32.55	16.37
110	-31.63	16.61
120	-30.83	16.80
150	-29.03	17.14
200	-27.22	17.40
300	-25.27	17.57
400	-24.03	17.62
600	-22.21	17.65
800	-20.84	17.58
1000	-19.68	17.50
1173	-18.80	17.41
1332	-18.11	17.31
1500	-17.47	17.20
2000	-15.90	16.90
2500	-14.73	16.64
3000	-13.86	16.41

Table 10
Summary of systematic error bias as a function of energy for efficiency calibration.

Energy (keV)	Bias (%)			Total
	Hotspot	Package Mass	Material composition	
45	-38,9	0,0	-7,4	-46,3
50	-38,4	0,0	-6,6	-45,0
60	-37,3	0,0	-4,9	-42,2
70	-36,1	0,0	-5,1	-41,2
80	-34,8	0,0	-5,8	-40,6
90	-33,6	0,0	-6,5	-40,2
100	-32,6	0,0	-7,0	-39,6
110	-31,6	0,0	-7,3	-38,9
120	-30,8	0,0	-7,3	-38,2
150	-29,0	0,0	-7,3	-36,4
200	-27,2	0,0	-6,7	-33,9
300	-25,3	0,0	-6,4	-31,7
400	-24,0	0,0	-6,3	-30,3
600	-22,2	0,0	-5,7	-28,0
800	-20,8	0,0	-5,2	-26,0
1000	-19,7	0,0	-4,7	-24,4
1500	-17,5	0,0	-4,4	-21,8
2000	-15,9	0,0	-4,2	-20,1
2500	-14,7	0,0	-4,2	-18,9
3000	-13,9	0,0	-4,1	-18,0

Table 11
Summary of uncertainty (1σ) as a function of energy for efficiency calibration.

Energy (keV)	Standard deviation (%)			
	Hotspot	Package Mass	Material composition	Total
45	13,9	5,0	13,1	19,7
50	14,2	5,0	12,8	19,7
60	14,7	5,0	11,9	19,5
70	15,2	5,0	10,5	19,1
80	15,6	5,0	9,0	18,7
90	16,0	5,0	7,6	18,4
100	16,4	5,0	6,4	18,3
110	16,6	5,0	5,3	18,1
120	16,8	5,0	4,5	18,1
150	17,1	5,0	2,6	18,0
200	17,4	5,0	1,0	18,1
300	17,6	5,0	0,2	18,3
400	17,6	5,0	0,4	18,3
600	17,7	5,0	0,6	18,4
800	17,6	5,0	0,6	18,3
1000	17,5	5,0	0,6	18,2
1500	17,2	5,0	0,6	17,9
2000	16,9	5,0	0,5	17,6
2500	16,6	5,0	0,3	17,4
3000	16,4	5,0	0,2	17,2

The method described in this paper can easily be used for other waste types in other laboratories worldwide.

Declaration of competing interest

The authors declare that they have no known competing financial interests or personal relationships that could have appeared to influence the work reported in this paper.

Acknowledgements

The authors would like to thank Biagio Zaffora and Régis Michaud for the fruitful discussions and feedback on this study.

References

- Aitchison, J., 2003. *The Statistical Analysis of Compositional Data*. Chapman & Hall, Publication, London (UK).
- Bosko, A., Mena, N., Spillane, T., Bronson, F., Venkataraman, R., Russ, W.R., Mueller, W., Nizhnik, V., 2011. Efficiency optimization employing random and smart search using multiple counts and line activity consistency benchmarks. In: *Proceedings of WM2011 Conference (Phoenix, AZ)*.
- Bronson, F., October 1997. ISOCS, a laboratory quality Ge gamma spectroscopy system you can take to the source for immediate high quality results. In: *Proceedings of the Rapid Radioactivity Measurements in Emergency and Routine Situations Conference*. UK.
- Carrel, F., et al., Aug. 2014. Characterization of old nuclear waste packages coupling photon activation analysis and complementary non-destructive techniques. *IEEE Trans. Nucl. Sci.* 61 (Issue: 4).
- Dumazert, J., et al., 21 February 2020. Inverse Problem Approach for the underwater localization of Fukushima Daiichi fuel debris with fission chambers. *Nucl. Instrum. Methods* 954, 161347.
- Frosio, T., Mena, N., Bertreix, P., Rimlinger, M., February. Theis. A novel technique for the optimization and reduction of gamma spectroscopy geometry uncertainties. *Appl. Radiat. Isot.*, Volume156, 108953. doi:<https://doi.org/10.1016/j.apradiso.2019.108953>.
- Frosio, T., Mena, N., Duchemin, C., Riggaz, N., Theis, C., January 2020. A new gamma spectroscopy methodology based on probabilistic uncertainty estimation and conservative approach. *Appl. Radiat. Isot.* 55.
- Frosio, T., Magistris, M., Mena, N., Michaud, R., Rimlinger, M., Theis, C., 2020b. Radiological characterization of large electromagnets in view of their elimination as very low-level wastes. *Nucl. Instrum. Methods Phys. Res.*
- Hijazi, R.H., Jernigan, R.W., 2009. Modelling compositional data using Dirichlet regression models. *J. Appl. Prob. Stat.* 4 (1), 77–91.
- GUM 1995, *Evaluation of Measurement Data — Guide to the Expression of Uncertainty in Measurement*, 2008. Publication.
- N. Mena et al.: "Mathematical Efficiency Calibration with Uncertain Source Geometries Using Smart Optimization", 2011 2nd International Conference on Advancements in Nuclear Instrumentation, Measurement Methods and Their Applications.
- Narayanan, A., Nov. 1992. A note on parameter estimation in the multivariate beta distribution. *Computer & Mathematics with applications* 24, 11–17.
- Rodrigues, L.A., et al. Pawlowsky-Glahn, V., Buccianti, A., 2011. *Compositional Data Analysis: Theory and Applications*. Publisher: John Wiley & Sons, London.
- Spillane, T., Mena, N., Atrashkevich, V., Bosko, A., Bronson, F., Nakazawa, D., Russ, W. R., Venkataraman, R., August 2010. An adaptive approach to mathematical efficiency calibration with uncertain source geometries. In: *Proceedings of the American Nuclear Society Topical Meeting on Decommissioning, Decontamination and Reutilization*. Idaho Falls, ID USA.
- IEEE standard test procedures for germanium gamma-ray detectors. DOI 10.1109/IEEESTD.1997.82400.
- Venkataraman, R., Bronson, F., Atrashkevich, V., Field, M., Young, B.M., 2003. Improved detector response characterization method in ISOCS and LabSOCS. In: *Methods and Applications of Radioanalytical Chemistry (MARC VI) Conference*.